Enhanced light-conversion efficiency of titanium-dioxide dye-sensitized solar cells with the addition of indium-tin-oxide and fluorine-tin-oxide nanoparticles in electrode films

Tammy P. Chou, Qifeng Zhang, Bryan Russo, and Guozhong Cao
Department of Materials Science and Engineering, University of Washington, 302 Roberts Hall, Box 352120, Seattle, WA 98195, U.S.A.
gzcao@u.washington.edu

Abstract. We prepared of electrodes that consist of TiO_2 with addition of tin-doped indium oxide (ITO) or fluorine-doped tin oxide (FTO) nanoparticles and the application of such electrodes on dye-sensitized solar cell. As compared to TiO_2 alone, the addition of ITO and FTO nanoparticles resulted in an efficiency improvement of ~ 20% up to ~ 54% for the TiO_2-ITO and TiO_2-FTO systems, respectively. This improvement was partly attributed to a slightly enhanced dye-adsorption behavior and a change in the TiO_2 surface chemistry due to the presence of ITO or FTO nanoparticles.

Keywords: dye-sensitized solar cell, nanoparticle, electrode film, light-conversion efficiency

1 INTRODUCTION

There have been many studies on dye-sensitized TiO_2 solar cells with the addition of SnO_2, ZnO, or Nb_2O_5 in combination with TiO_2 to form heterostructure films in order to reduce recombination losses through surface recombination of electrons and holes [1-15]. In addition, heterojunction structures comprised of a semiconducting oxide in combination with an insulating oxide have been studied to modify the surface chemistry through pH changes to enhance the adsorption of the sensitizer dye [16, 17]. However, to this point, there have been no studies on the fabrication of TiO_2-ITO (Indium-Tin-Oxide) or TiO_2-FTO (Fluorine-Tin-Oxide) film electrodes for the application of solar cells. By incorporating ITO or FTO nanoparticles into the TiO_2 nanoparticle film, it is assumed that the charge transport properties, or the internal resistance, would improve through the use of materials with higher conductivity, resulting in higher short-circuit current density and overall efficiency. This assumption is based on ITO and FTO having much higher electron mobilities ~ 40-70 cm^2/Vs [18] and ~ 19 cm^2/Vs [19], as compared to the electron mobility of anatase TiO_2 with a value ~ 10^{-5} cm^2/Vs [20].

Here, we describe solar cells with films combining the properties of TiO_2 and ITO or FTO to enhance the overall light conversion efficiency of dye-sensitized TiO_2 solar cells. Films consisting of 1) TiO_2 nanoparticles, 2) TiO_2 nanoparticles with the addition of ITO nanoparticles, and 3) TiO_2 nanoparticles with the addition of FTO nanoparticles were fabricated and analyzed in order to compare the resultant overall light conversion efficiencies. These films were studied in an attempt to determine the effects of adding a higher conducting ITO or FTO material into the TiO_2 system, either through the possible reduction of the internal resistance or the possible modification of the surface chemistry in the TiO_2 nanoparticle film. It was found that with the addition of ITO or FTO nanoparticles to the TiO_2 nanoparticle film electrode, the overall light conversion efficiency increased in both cases.

Received 11 Jul 2008; accepted 24 Nov 2008; published 1 Dec 2008 [CCC: 19342608/2008/$25.00]

2 EXPERIMENTS

From previously published work [21-23], TiO_2 nanoparticles in the anatase phase were obtained from TiO_2 sol by hydrothermal treatment at 250 °C for 20 minutes with diameters of ~ 18 nm. After that, the sol became a paste-like substance, which was then allowed to dry at 100 °C for 24 hours. The resultant pieces were ground into a fine powder for use.

ITO nanoparticles were prepared from precursor materials also by way of sol-gel processing, as previously reported [21-24], by combining ethylene glycol ($HOCH_2CH_2OH$, JT Baker, Phillipsburg, NJ), ethanol (C_2H_5OH, 200 proof, AAPER, Shelbyville, KY), citric acid ($HOC(CO_2H)(CH_2CO_2H)_2$, monohydrate, JT Baker, Phillipsburg, NJ), tin (IV) chloride ($SnCl_4$, 98%, anhydrous, Alfa Aesar, Ward Hill, MA), indium (III) chloride ($InCl_3$, 99.99%, anhydrous, Alfa Aesar, Ward Hill, MA), and DI-H_2O with a nominal molar ratio of $1.00:1.42:6.67x10^{-2}:3.34x10^{-3}:3.06x10^{-2}:3.61x10^{-2}$, respectively. In short, citric acid and $SnCl_4$ were added to a mixture of ethylene glycol and ethanol, and stirred at a rate of 500 RPM at 40 °C for 60 minutes. An amount of $InCl_3$ was then added and stirred for another 90 minutes at 40 °C; DI-H_2O was added 45 minutes into the stirring. The nanoparticle powder formed from ITO sol was obtained by first drying 20 mL of ITO sol in a crucible at 100 °C for 24 hours in air and then sintering at 700 °C for 1 hour at a heating rate of 2 °C/min. The resultant ITO powder obtained was then ground down to smaller particles using a mortar and pestle.

FTO nanoparticles were prepared by way of solution methods, as previously reported [25,26]. In short, 10.5g of tin (IV) chloride pentahydrate ($SnCl_4 \bullet 5H_2O$, 98%, Sigma-Aldrich, St. Louis, MO) was added to 150 mL ethanol (C_2H_5OH, 200 proof, AAPER, Shelbyville, KY) and mixed in a sealed glass vial for ~ 5 hours. In another sealed glass vial, 1.86 g ammonium fluoride (NH_4F, 98%, Sigma-Aldrich, St. Louis, MO) was added to 5.04mL DI-H_2O and mixed for ~ 5 hours. The fluoride solution was then added to the glass vial containing the tin chloride solution while in a water bath at 60°C temperature. A clear solution was obtained after a white precipitate formed and redissolved in solution. The FTO nanoparticles were obtained by slowly adding dropwise FTO solution into a crucible at 440 °C. A brownish crust could be observed on the bottom of the crucible. After enough FTO was obtained, a final sintering process was performed at 440 °C for ~ 1 hour. The resultant obtained FTO pieces was then ground to finer particles using a mortar and pestle. XRD data showed that ITO nanoparticles and FTO nanoparticles ranging from ~ 10 nm to ~ 15 nm diameters were obtained.

For solar cell assembling, electrode films consisting of TiO_2 nanoparticles and ITO or FTO nanoparticles were directly deposited onto conductive fluorine-tin-oxide (FTO, TCO10-10, R_s ~ 10 ohm/sq, Solaronix SA, Switzerland) coated glass substrates using previously reported methods [11]. In summary, a dispersion of 20-30 wt% powder in a 1:1 ratio of DI-H_2O to ethanol solution was doctor-bladed on the surface of the FTO substrates after hydrolyzing at 90-100 °C in DI-H_2O for 30-60 minutes. The films were then dried in air at 100 °C for 1 hour, and sintered at 500 °C for 1 hour at a heating rate of 2 °C/min. The sintered films were all sensitized by heating to 70 °C and subsequently immersing in standard ruthenium-based red (N3), cis-bis-(isothiocyanato)-bis-(2,2'-bipyridyl-4,4'-dicarboxylato)-ruthenium(II) (Solterra Fotovoltaico SA, Switzerland), with a concentration close to $5x10^{-4}$ M in ethanol for ~ 12 hours for dye adsorption. A Pt-coated silicon substrate with a Pt layer thickness of ~ 180 nm was used as the counter electrode. An iodide-based solution was used as the liquid electrolyte, consisting of 0.6 M tetra-butylammonium iodide (Sigma-Aldrich, St Louis, MO), 0.1 M lithium iodide (LiI, Sigma-Aldrich, St Louis, MO), 0.1 M iodine (I_2, Sigma-Aldrich, St Louis, MO), and 0.5 M 4-tert-butyl pyridine (Sigma-Aldrich, St Louis, MO) in acetonitrile (Mallinckrodt Baker, Phillipsburg, NJ).

Electrical characteristics and photovoltaic properties of each solar cell were measured and calculated using simulated AM1.5 sunlight illumination with 100 mW/cm^2 light output. All the I-V curves of the solar cells were obtained in the dark and under illumination, where a

range from -0.3 V to 2 V was used during each measurement. The I-V characteristics as a function of the incident light intensity was used to obtain the open-circuit voltage (V_{oc}), short-circuit current density (J_{sc}), the maximum voltage point (V_{max}), and the maximum current density point (J_{max}). Multiple samples were tested for each type of film, resulting in reproducible results with slight deviations in the short-circuit current (~ ±0.05 mA), open-circuit voltage (~ ±10 mV), and the light conversion efficiency (~ ±0.02%).

The amount of dye adsorbed was determined for all the nanoparticle powders and films using the method of dye elution. For the TiO_2, ITO, and FTO powders and films, approximately 0.02g of each was each immersed in 5 mL of N3 dye for ~ 24 hours. For the TiO_2-ITO and TiO_2-FTO powders and films, approximately 0.012 g of TiO_2 was intermixed with 0.004 g of ITO or FTO and immersed in 5 mL of N3 dye for ~ 24 hours. The immersed powders were separated from the dye solution by centrifugation for ~ 2 minutes, and the immersed films were directly removed to analyze the resultant dye solution after dye adsorption. The intensity of the absorption peak of the resultant dye solution after dye adsorption was compared to the absorption peak of the initial N3 dye solution with a concentration of ~ 1.25×10^{-6} M in ethanol to determine the number of moles adsorbed.

The zeta potential (ZetaPALS, Brookhaven Instruments Ltd, UK) of the nanoparticle powders were also analyzed to determine any changes to the surface chemistry of the TiO_2 nanoparticle powders with the addition of ITO or FTO nanoparticles. Each powder was dispersed in a solution of ethanol with a very low concentration so as the solution remained fairly clear even with a dispersion of particles. Each sample was analyzed for five 15-cycle runs under a current of 1.2 mA and an electric field of 14.31 V/cm, and the average particle mobility was used to calculate the average zeta potential with standard error.

3 RESULTS AND DISCUSSION

The TiO_2 films containing additional ITO or FTO nanoparticles with different amount as 5 wt%, 10 wt%, 15 wt%, 20 wt% and more were studied. The result showed a 20 wt% addition amount could offer the best effect on the enhancement of solar-to-electricity conversion efficiency. Fig. 1 compares the I-V behavior of each type of nanoparticle film worked as solar cell electrode. Table 1 summarizes the short-circuit current density, the open-circuit voltage, the fill factor, and the overall light conversion efficiency of all films. It can be seen that the solar cell consisting of the TiO_2 nanoparticle film electrode resulted in a short-circuit current density of ~ 13 mA/cm^2 and an overall efficiency of ~ 4.7%. With the addition of ITO nanoparticles into the TiO_2 nanoparticle film electrode, it was found that the short-circuit current density increased from ~ 13 mA/cm^2 to ~ 15 mA/cm^2 and that the overall efficiency increased from ~ 4.7% to 5.6%, resulting in a ~ 20% improvement in both the short-circuit current density and the overall efficiency. A further increase in the short-circuit current density and the overall efficiency resulted from the addition of FTO nanoparticles into the TiO_2 nanoparticle film electrode. The short-circuit current density and the overall efficiency increased from ~ 13 mA/cm^2 to ~ 23 mA/cm^2, and from ~ 4.7% to 7.2%, resulting in a much higher ~ 78% and ~ 54% improvement, respectively.

There are a few possible factors for the improvement in the short-circuit current density and the overall light conversion efficiency with the addition of ITO or FTO nanoparticles to the TiO_2 nanoparticle film. These possible factors include: 1) the presence of clustered ITO or FTO nanoparticles in the submicron range to promote light-scattering, 2) the reduction of the internal resistance with the presence of higher conducting ITO or FTO nanoparticles to improve the electron transport properties, 3) the enhancement of the dye adsorption behavior with the addition of ITO or FTO nanoparticles, and 4) the change in the surface chemistry with the addition of ITO or FTO nanoparticles to reduce the likelihood of charge recombination.

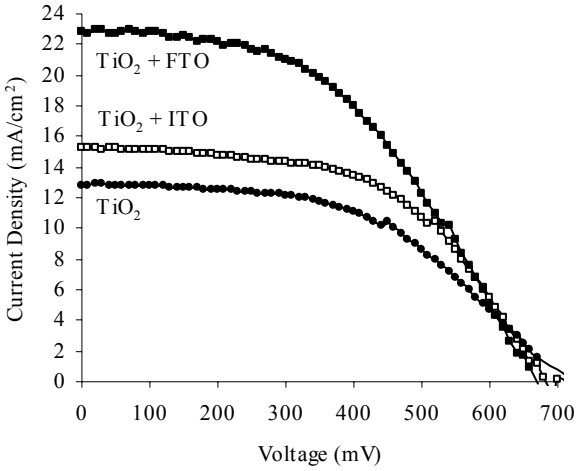

Fig. 1. Plot of the I-V behavior of TiO_2 (●), TiO_2-ITO (□), and TiO_2-FTO (■) film electrodes in dye-sensitized solar cells under 100 mW/cm^2 illumination.

Table 1. Summary of values for TiO2, TiO2-ITO, and TiO2-FTO film electrodes found from solar cell analysis, as seen in Fig. 1.

Film	**V_{oc} (mV)**	**J_{sc} (mA/cm^2)**	**V_{max} (mV)**	**J_{max} (mA/cm^2)**	**FF (%)**	**η (%)**
TiO_2	700	12.8	450	10.4	52.2	4.7
TiO_2 + ITO	690	15.3	450	12.5	53.1	5.6
TiO_2+ FTO	670	22.8	400	18.0	47.2	7.2

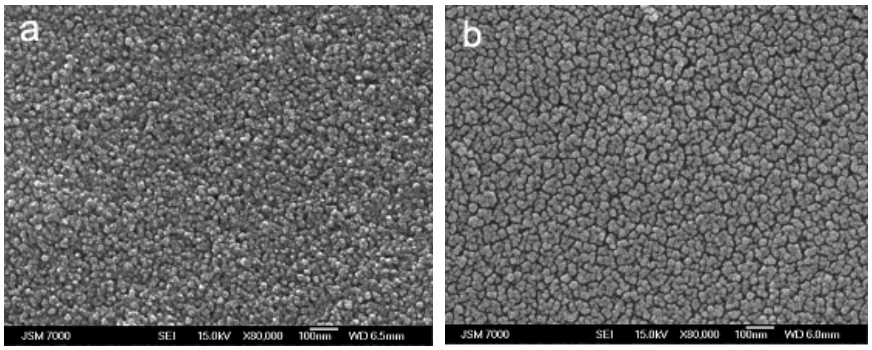

Fig. 2. SEM images of the a) TiO2 and b) TiO2-ITO film electrodes tested in dye-sensitized solar cells. The SEM image of the TiO2-FTO film electrode is not shown, as it is similar to the SEM image of the TiO2-ITO film electrode.

Further analysis, however, did not verify some of the possible factors described above. Additional SEM analysis on the TiO_2, TiO_2-ITO, and TiO_2-FTO films, as shown in Fig. 2, showed that large clusters were not visible as initially thought. The TiO_2 film structures with and without the addition of ITO or FTO were only slightly different in that small clustering was found for the TiO_2-ITO and TiO_2-FTO films but was not present for the TiO_2 films.

Initially, it was thought that large clustering of the ITO or FTO nanoparticles may have occurred during the processing steps and these clusters may have been incorporated into the TiO_2 film, which may have possibly promoted light-scattering events [27-30]. But from the SEM images, it can be seen that small clusters less than 100nm (the minimum size necessary to promote light-scattering) were formed that are not in the sub-micron range. The absence of large sub-micron clusters in the TiO_2-ITO film indicate that light-scattering was not a factor in the improvement in the short-circuit current density and the overall conversion efficiency, and that other factors may have played a role.

Based on the fill factor values, it can also be assumed that the reduction in the internal resistance was not a factor for the improvement in the short-circuit current density and the overall conversion efficiency. The fill factor slightly varied within a ~ 6% range from ~ 52% to ~ 53% to ~ 47% for the TiO_2, TiO_2-ITO, and TiO_2-FTO film electrodes, respectively. Since this difference is very small, the addition of ITO or FTO nanoparticles to the TiO_2 nanoparticle film did not affect the internal resistance, which was initially thought to be influenced by the use of higher conducting ITO or FTO nanoparticles to improve the electron transport properties. The similarity in the fill factor for the three types of film electrodes can also be depicted by the similarity found from the curvature of the I-V plots in Fig. 1.

One aspect that may have influenced the short-circuit current density and the overall conversion efficiency is the difference in the dye adsorption behavior of the TiO_2 nanoparticle film with and without the addition of ITO or FTO nanoparticles, similar to the report previously mentioned by Jung et al. [16] and Bandaranayake et al. [17] A higher amount of dye adsorbed on the surface would generate a greater number of electron-hole pairs by absorbing more of the incident light, resulting in a higher short-circuit current density and thus a higher overall light conversion efficiency. This concept was studied by measuring the amount of dye adsorbed on each type of nanoparticle film and comparing the amount of dye adsorbed to the resultant short-circuit current density and overall conversion efficiency. Figure 3 compares the adsorption behavior, the short-circuit current density, and the overall efficiency for the TiO_2, TiO_2-ITO, and TiO_2-FTO nanoparticle films.

It can be seen that the amount of dye adsorbed increased with the addition of ITO or FTO nanoparticles. The TiO_2-FTO nanoparticle film electrode had the highest amount of dye adsorption, followed by the TiO_2-ITO and the TiO_2 nanoparticle film electrodes, respectively. The short-circuit current density and the overall efficiency also followed the same trend. The amount of dye adsorbed for the TiO_2, TiO_2-ITO, and TiO_2-FTO nanoparticle films were estimated to be ~ 44 mmol/kg, ~ 48 mmol/kg, and ~ 49 mmol/kg, respectively. The improvement in the dye adsorption behavior was much lower than the improvement in the short-circuit current density and in the overall efficiency.

With the addition of ITO nanoparticles, the dye adsorption improved by ~ 9%, but the short-circuit current density and the overall conversion efficiency both improved by a larger margin of ~ 20%. With the addition of FTO, the dye adsorption behavior improved by ~ 11%, but the short-circuit current density and the overall efficiency improved by a much larger margin of ~ 78% and ~ 54%, respectively. The disproportioned improvement in the dye adsorption in comparison with the short-circuit current density and the overall conversion efficiency indicates that the improved dye adsorption behavior has partial contribution to the enhanced short-circuit current density and the overall efficiency, and that other factors may have also influenced these results.

Furthermore, with the slight change in the dye adsorption behavior, as well as the slight deviation in the open-circuit voltage within a ~ 30 mV range, a slight change in the surface

chemistry may have occurred with the addition of ITO or FTO nanoparticles to the TiO_2 nanoparticle film. Figure 3 shows the dye adsorption and zeta potential of the TiO_2, TiO_2-ITO, and TiO_2-FTO nanoparticle systems. Table 2 summarizes the dye adsorption and the zeta potential values for the TiO_2, TiO_2-ITO, and TiO_2-FTO, ITO, and FTO nanoparticle systems. The dye adsorption was tested for each nanoparticle system in powder form to correlate with each powder dispersion used to determine the zeta potential for better comparison. It should also be noted that the dye adsorption values are lower in film form than in powder form due to possible weight loss from nanoparticle removal during film processing and preparation.

The plot in Fig. 4 shows a similar trend in the increase in the dye adsorption behavior as that shown in Fig. 3, where the TiO_2-FTO nanoparticle system had the highest amount of dye adsorption, followed by the TiO_2-ITO and the TiO_2 nanoparticle systems, respectively. The amount of dye adsorbed for the TiO_2, TiO_2-ITO, and TiO_2-FTO nanoparticle systems were estimated to be ~ 56 mmol/kg with a standard deviation of ~ 0.2 mmol/kg, ~ 57 mmol/kg with a standard deviation of ~ 0.4 mmol/kg, and ~ 58 mmol/kg with a standard deviation of ~ 0.3 mmol/kg, respectively. The addition of ITO or FTO nanoparticles to the TiO_2 nanoparticle system only slightly improved the dye adsorption by ~ 2% and ~ 4%, respectively. A possible reason is from the increase in the surface roughness due to the addition of ITO or FTO nanoparticles and therefore the available surface for dye adsorption.

It can also be seen that the trend for the zeta potential is reversed, as compared to that for the dye adsorption. The TiO_2 nanoparticle system had the highest zeta potential, followed by the TiO_2-ITO and the TiO_2-FTO nanoparticle systems, respectively. The zeta potential of the TiO_2 nanoparticle system was determined to be ~ 40 mV with a standard error of ~ 1 mV. With the addition of ITO nanoparticles to the TiO_2 nanoparticle system, the zeta potential decreased to ~ 34 mV with a standard error of ~ 2 mV. A further decrease to ~ 27 mV with a standard error of ~ 2 mV in the zeta potential was found with the addition of FTO nanoparticles to the TiO_2 nanoparticle system.

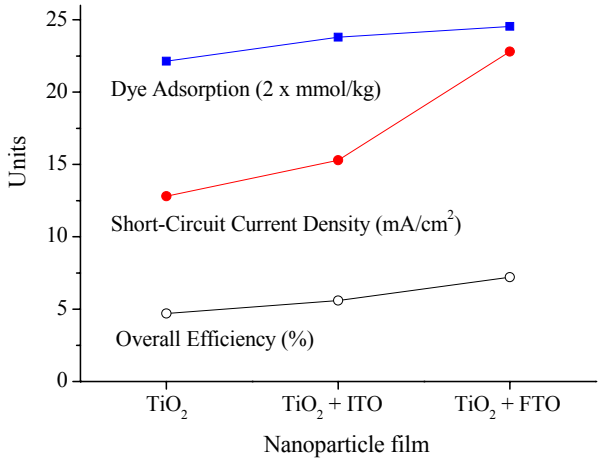

Fig. 3. Comparison of the amount of dye adsorbed (■), the relative short-circuit current density (●), and the relative overall efficiency (○) for the TiO_2, TiO_2-ITO, and TiO_2-FTO film electrodes.

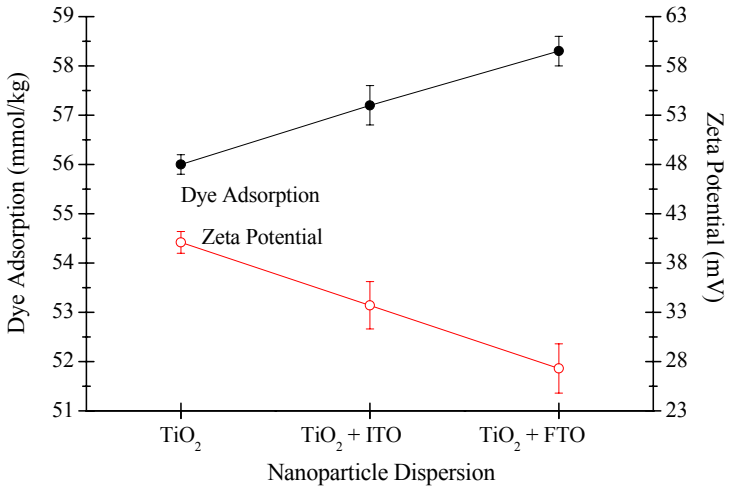

Fig. 4. Comparison of the amount of dye adsorbed (●) to the zeta potential (○) for the TiO2, TiO2-ITO, and TiO2-FTO nanoparticle systems. The vertical bars denote the error of measured data. The dye adsorption was determined for each mixture of nanoparticle powder, and the zeta potential was determined for each nanoparticle dispersion in ethanol.

Table 2. Summary of dye adsorption and zeta potential values for the TiO2, TiO2-ITO, TiO2-FTO, ITO, and FTO nanoparticle systems.

Nanoparticle Systems	**Dye Adsorption (mmol/kg)**	**Average Zeta Potential (mV)**
TiO_2	56.0 ± 0.2	40.1 ± 1.1
TiO_2 + ITO	57.2 ± 0.4	33.7 ± 2.4
TiO_2 + FTO	58.3 ± 0.3	27.3 ± 2.5
ITO	1.6 ± 0.2	31.5 ± 1.6
FTO	7.2 ± 0.2	22.3 ± 3.9

Table 2 summaries of the dye adsorption and zeta potential values for the TiO_2, TiO_2-ITO, TiO_2-FTO, ITO, and FTO nanoparticle systems. It should be noted that the much lower estimated dye adsorption values of ~ 1.6 mmol/kg with a standard deviation of ~ 0.2 mmol/kg and ~ 7.2 mmol/kg with a standard deviation of ~ 0.2 mmol/kg associated with the ITO and FTO nanoparticle systems alone, respectively, show that the amount of dye adsorbed on the ITO and FTO nanoparticles was not a factor in the increase in the amount of dye adsorbed for the TiO_2-ITO and TiO_2-FTO nanoparticle systems. The ITO nanoparticle film also showed much lower dye adsorption; however, the dye adsorption was not obtained for the FTO nanoparticle film since this film could not be prepared in the same manner for comparison.

The addition of ITO or FTO nanoparticles, with their lower individual zeta potentials, may have had an influence on the surface chemistry or the ionic character of the TiO_2 nanoparticle system. The lowering of the zeta potential may indicate the change in the surface chemistry, or ionic character, and may be a cause in the enhancement of the short-circuit current density and overall conversion efficiency through the reduction of charge

recombination losses. However, it is inconclusive as to the mechanism of surface chemistry changes by the addition of ITO or FTO nanoparticles, and its affect on the short-circuit current density and overall conversion efficiency.

Furthermore, it is unknown exactly what influence the addition of ITO or FTO nanoparticles has on the TiO_2 nanoparticle system, beyond the dye adsorption behavior and the zeta potential. Therefore, further examination on the changes in the surface chemistry or the ionic characteristic of the TiO_2 nanoparticles with the addition of ITO or FTO nanoparticles are needed to further understand the effect of the zeta potential on the dye adsorption and the overall efficiency. Additional studies on the effect of the addition of ITO or FTO nanoparticles on the electron transport properties of TiO_2 nanoparticles are also needed to fully contemplate whether the differences in the short-circuit current density and the overall light conversion efficiency are also partly affected by the internal resistance and the efficiency of electron transport, even though differences in the fill factor were not seen.

3 CONCLUSIONS

In conclusion, it was found that the addition of ITO or FTO nanoparticles to the TiO_2 nanoparticle system in the fabrication of film electrodes for dye-sensitized solar cells resulted in an improvement in the short-circuit current density and in the overall conversion efficiency. The short-circuit current density improved by ~ 20% and ~ 78% with the addition of ITO and FTO, respectively; the overall conversion efficiency also improved by ~ 20% and ~ 54% with the addition of ITO and FTO, respectively. This increase was assumed to be possibly due to four factors: 1) light-scattering, 2) reduced internal resistance, 3) enhanced dye adsorption, and 4) surface chemistry changes. Further analysis showed that light-scattering and reduced internal resistance were not factors based on the presence of small clusters and similar fill factors for all three nanoparticle systems, respectively. However, it was found that the increase in the short-circuit current density and the overall efficiency were partly caused by the change in the dye adsorption behavior and the change in the surface chemistry with the addition of ITO or FTO nanoparticles, as evidenced by the change in the zeta potential values. The TiO_2-FTO, TiO_2-ITO, and TiO_2 nanoparticle systems with a low to high zeta potential showed a high to low amount of dye adsorption, respectively.

Acknowledgments

Financial support by the UW-PNNL Joint Institute for Nanoscience (JIN) and the Intel Ph.D. Foundation; and the Air Force Office of Scientific Research (AFOSR-MURI, FA9550-06-1-032) and the Department of Energy (DE-FG02-07ER46467). Acknowledgement to Professor Samson Jenekhe and Dr. Abhishek Pradeep Kulkarni for the use of their lab and solar cell testing equipment.

References

[1] S. Chappel, S. G. Chen, and A. Zaban, "TiO_2-coated nanoporous SnO_2 electrodes for dye-sensitized solar cells," *Langmuir* **18**, 3336-3342 (2002) [doi:10.1021/la015536s].

[2] S. Chappel and A. Zaban, "Nanoporous SnO_2 electrodes for dye-sensitized solar cells: improved cell performance by the synthesis of 18 nm SnO_2 colloids," *Sol. Energ. Mater. Sol. Cells* **71**, 141-152 (2002) [doi:10.1016/S0927-0248(01)00050-2].

[3] K. Tennakone, P. K. M. Bandaranayake, P. V. V. Jayaweera, A. Konno, and G. R. R. A. Kumara, "Dye-sensitized composite semiconductor nanostructures," *Physica E* **14**, 190-196 (2002) [doi:10.1016/S1386-9477(02)00382-X].

[4] K. M. P Bandaranayake, M. K. Indika Senevirathna, P. M. G. M. Prasad Weligamuwa, and K. Tennakone, "Dye-sensitized solar cells made from

nanocrystalline TiO_2 films coated with outer layers of different oxide materials," *Coord. Chem. Rev.* **248**, 1277-1281 (2004) [doi:10.1016/j.ccr.2004.03.024].

[5] T. Stergiopoulos, I. M. Arabatzis, M. Kalbac, I. Lukes, and P. Falaras, "Incorporation of innovative compounds in nanostructured photoelectrochemical cells," *J. Mater. Proc. Tech.* **161**, 107-112 (2005) [doi:10.1016/j.jmatprotec.2004.07.014].

[6] S. G. Chen, S. Chappel, Y. Diamant, and A. Zaban, "Preparation of Nb_2O_5 coated TiO_2 nanoporous electrodes and their application in dye-sensitized solar cells," *Chem. Mater.* **13**, 4629-4634 (2001) [doi:10.1021/cm010343b].

[7] T. S. Kang, S. H. Moon, and K. J. Kim, "Enhanced photocurrent-voltage characteristics of Ru(II)-dye sensitized TiO_2 solar cells with TiO_2-WO_3 buffer layers prepared by a sol-gel method," *J. Electrochem. Soc.* **149**, E155-E158 (2002) [doi:10.1149/1.1467367].

[8] K. Keis, C. Bauer, G. Boschloo, A. Hagfeldt, K. Westermark, H. Rensmo, and H. Siegbahn, "Nanostructured ZnO electrodes for dye-sensitized solar cell applications," *J. Photochem. Photobiol. A: Chem.* **148**, 57-64 (2002) [doi:10.1016/S1010-6030(02)00039-4].

[9] A. B. Kashyout, M. Soliman, M. El Gamal, and M. Fathy, "Preparation and characterization of nano particles ZnO films for dye-sensitized solar cells," *Mater. Chem. Phys.* **90**, 230-233 (2005) [doi:10.1016/j.matchemphys.2004.11.031].

[10] D. Menzies, Q. Dai, Y.B. Cheng, G. P. Simon, and L. Spiccia, "Improvement of the Zirconia shell in nanostructured titania core-shell working electrodes for dye-sensitized solar cells," *Mater. Lett.* **59**, 1893-1896 (2005) [doi:10.1016/j.matlet.2005.02.048].

[11] D. B. Menzies, L. Bourgeois, Y. B. Cheng, G. P. Simon, N. Brack, and L. Spiccia, "Characterization of nanostructured core-shell working electrodes for application in dye-sensitized solar cells," *Surf. Coat. Tech.* **198**, 118-122 (2005) [doi:10.1016/j.surfcoat.2004.10.110].

[12] S. Chappel, L. Grinis, A. Ofir, and A. Zaban, "Extending the current collector into the nanoporous matrix of dye sensitized electrodes," *J. Phys. Chem. B Lett.* **109**, 1643-1647 (2005).

[13] Y. Diamant, S. Chappel, S. G. Chen, O. Melamed, and A. Zaban, "Core-shell nanoporous electrode for dye sensitized solar cells: the effect of shell characteristics on the electronic properties of the electrode," *Coord. Chem. Rev.* **248**, 1271-1276 (2004) [doi:10.1016/j.ccr.2004.03.003].

[14] E. Palomares, J. N. Clifford, S. A. Haque, T. Lutz, and J. R. Durrant, "Control of charge recombination dynamics in dye sensitized solar cells by the use of conformally deposited metal oxide blocking layers," *J. Amer. Chem. Soc.* **125**, 475-482 (2003) [doi:10.1021/ja027945w].

[15] J. Bandara, U. W. Pradeep, and R. G. S. J. Bandara, "The role of n-p junction electrodes in minimizing the charge recombination and enhancement of photocurrent and photovoltage in dye sensitized solar cells," *J. Photochem. Photobiol. A: Chem.* **170**, 273-278 (2005) [doi:10.1016/j.jphotochem.2004.08.023].

[16] H. S. Jung, J-K. Lee, M. Nastasi, S-W. Lee, J-Y. Kim, J-S. Park, K. S. Hong, and H. Shin, "Preparation of nanoporous MgO-Coated TiO_2 nanoparticles and their application to the electrode of dye-sensitized solar cells," *Langmuir* **21**, 10332-10335 (2005) [doi:10.1021/la051807d].

[17] P. K. M. Bandaranayake, P. V. V. Jayaweera, and K. Tennakone, "Dye-sensitization of magnesium-oxide-coated cadmium sulfide," *Sol. Energ. Mater. Sol. Cells* **76**, 57-64 (2003) [doi:10.1016/S0927-0248(02)00249-0].

[18] D. Mergel, M. Schenkel, M. Ghebre, and M. Sulkowski, "Structural and electrical properties of In_2O_3: Sn films prepared by radio-frequency sputtering," *Thin Solid Films* **392**, 91-97 (2001) [doi:10.1016/S0040-6090(01)01013-6].
[19] J. W. Bae, S. W. Lee, and G. Y. Yeom, "Doped-fluorine on electrical and optical properties of tin oxide films grown by ozone-assisted thermal CVD," *J. Electrochem. Soc.* **154**, D34-D37 (2007) [doi:10.1149/1.2382346].
[20] Th. Dittrich, E. A. Lebedev, and J. Weidmann, "Electron drift mobility in porous TiO_2 (anatase)," *Rap. Res. Notes* **165**, R5-R6 (1998).
[21] T. P. Chou, B. Russo, Q. F. Zhang, G. E. Fryxell, and G. Z. Cao, "Titania particle size effect on the overall performance of dye-sensitized solar cells," *J. Phys. Chem. C* **111**, 6296-6302 (2007) [doi:10.1021/jp068939f].
[22] S. J. Limmer, S. V. Cruz, and G. Z. Cao, "Films and nanorods of transparent conducting oxide ITO by a citric acid sol route," *Appl. Phys. A* **79**, 421-424 (2004) [doi:10.1007/s00339-004-2738-3].
[23] S. J. Limmer, S. Seraji, M. J. Forbess, Y. Wu, T.P. Chou, C. Nguyen, and G. Z. Cao, "Template-based growth of various oxide nanorods by sol-gel electrophoresis," *Adv. Funct. Mater.* **12**, 59-64 (2002) [doi:10.1002/1616-3028(20020101)12:1<59::AID-ADFM59>3.0.CO;2-B].
[24] T. L. Wen, J. Zhang, T.P. Chou, S.J. Limmer, and G. Z. Cao, "Template-based growth of oxide nanorod arrays by centrifugation," *J. Sol-Gel Sci. Tech.* **33**, 193-200 (2005).
[25] B. Russo and G. Z. Cao, "Fabrication and characterization of fluorine-doped thin oxide thin films and nanorod arrays via spray pyrolysis," *Appl. Phys. A* **90**, 311-315 (2008) [doi:10.1007/s00339-007-4274-4].
[26] A. E. Rakhshani, Y. Makdisi, and H. A. Ramazaniyan, "Electronic and optical properties of fluorine-doped tin oxide films," *J. Appl. Phys.* **83**, 1049-1057 (1998) [doi:10.1063/1.366796].
[27] G. Z. Cao, *Nanostructures & Nanomaterials: Synthesis, Properties, & Applications*, Imperial College Press, London (2004).
[28] T. P. Chou, Q. F. Zhang, G. E. Fryxell, and G. Z. Cao, "Hierarchically structured ZnO film for dye-sensitized solar cells with enhanced energy conversion efficiency," *Adv. Mater.* **19**, 2588-2592 (2007) [doi:10.1002/adma.200602927].
[29] Q. F. Zhang, T. P. Chou, B. Russo, S. A. Jenekhe, and G. Z. Cao, "Aggregation of ZnO nanocrystallites for high conversion efficiency in dye-sensitized solar cells," *Angew. Chem. Int. Ed.* **47**, 2402-2406 (2008) [doi:10.1002/anie.200704919].
[30] Q. F. Zhang, T. P. Chou, B. Russo, S. A. Jenekhe, and G. Z. Cao, "Polydisperse aggregates of ZnO nanocrystallites: a method for energy-conversion-efficiency enhancement in dye-sensitized solar cells," *Adv. Funct. Mater.* **18**, 1654-1660 (2008) [doi:10.1002/adfm.200701073].

Tammy P. Chou obtained her Ph. D. degree from University of Washington in 2006. Her research area involves the development and synthesis of various oxide materials in the nanoscale for the exploration of the chemistry and the nanostructure of various oxide electrodes for dye-sensitized solar cell applications.

Qifeng Zhang is currently a postdoctoral researcher in University of Washington. He received his Ph. D. degree from Peking University (China) in 2001. His research interests involve engineering applications of nano-structured materials on electrical devices including the solar cells, UV light-emitting diodes (LEDs), field-effect transistors (FETs), and gas sensors.

Bryan Russo was graduated from University of Washington with a Master degree in 2007. He studied the fabrication of fluorine-doped thin oxide thin films and nanorod arrays for solar cell applications.

Guozhong Cao is Boeing-Steiner Professor of Materials Science and Engineering at the University of Washington. He has published over 200 refereed papers, and authored and edited 4 books including "Nanostructures and Nanomaterials," and 3 conference proceedings on nanotechnology. His current research is focused mainly on nanomaterials for energy conversion and storage including solar cells, lithium-ion batteries, supercapacitors, and hydrogen storage materials.